

Optical spectra in condensed phases: how the medium polarizability affects charge-transfer dyes

D.K. Andrea Phan Huu, Cristina Sissa, Francesca Terenziani, and Anna Painelli*
Department of Chemistry, Life Science and Environmental Sustainability
 (Dated: March 21, 2022)

When designing molecular functional materials, the properties of the active specie, the dye, must be optimized fully accounting for environmental effects. Here we present an effective model to account for the spectroscopic effects of the medium electronic polarizability on the properties of charge-transfer dyes. Different classes of molecules are considered and the proposed antiadiabatic approach to solvation is contrasted with the adiabatic approach, currently adopted in all quantum chemical approaches to solvation. Transition frequencies and band-shapes are addressed, and the role of the medium polarizability on symmetry-breaking phenomena is also discussed.

I. INTRODUCTION

The effective design of molecular materials for innovative applications requires the concurrent optimization of the active specie, the dye, and its matrix, a highly non trivial task, since the molecular properties depend, in an intrinsically non-linear way, from the properties of the local environment. Charge transfer (CT) dyes composed of electron-donor (D) and acceptor (A) moieties connected by π -conjugated bridges find applications in solar cells,¹ OLED,^{2,3} non-linear optics,⁴⁻⁷ and are interesting model systems for photoinduced CT.^{8,9} The presence of low-lying excited states and of delocalized electrons makes these molecules extremely responsive to the local environment.¹⁰ Intermolecular interactions in aggregates, supramolecular complexes and crystals have been discussed in different contexts, underlying how mutually interacting polarizable and/or polar molecules lead to specific spectroscopic features that cannot be reconciled with the standard exciton models.¹¹⁻¹⁸ But even in comparatively simple systems, where the dye is dissolved in dilute solutions, in polymeric matrices or glasses, environmental effects may be quite impressive, ranging from the solvatochromism of polar dyes,^{19,20} to symmetry breaking phenomena²¹⁻²⁴

Essential-state models (ESMs) were proposed and successfully applied to describe low-energy spectral properties of CT dyes in different environments.^{10,14,21-23} ESMs are a family of parametric Hamiltonians that only account for few electronic molecular states, usually corresponding to the main resonating structures that characterize each dye, coupled to a few effective vibrational modes, to account for the geometry relaxation accompanying the CT process. After the success with dipolar D- π -A dyes,^{25,26} ESMs were applied to more complex quadrupolar and octupolar structures (see Fig. 1).^{21,22,27} The main asset of ESMs is the ability to rationalize in a single theoretical framework linear and non-linear optical spectra of the dyes, also addressing important and highly non-trivial environmental effects.

Limiting attention to the simplest environment, the solvent in a dilute solution, the most widely discussed effects are related to the solvent polarity.^{19,20,28} A po-

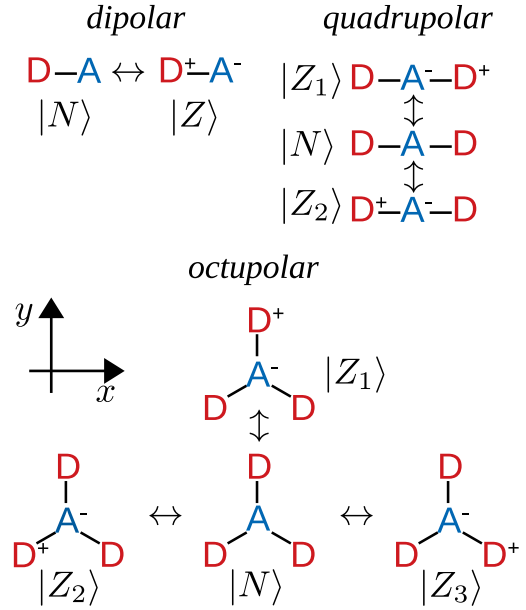


FIG. 1. Schematic representation of the main resonating structures of dipolar, quadrupolar and octupolar CT dyes.

lar solvent stabilizes the polar states of the solute, an effect related to the (re)orientation of the solvent molecules around the solute. Polar solvation is therefore related to slow degrees of freedom. The best known consequences of polar solvation are the solvatochromic effects in absorption and fluorescence spectra of polar dyes,^{19,20,26} as well as solvent-induced symmetry breaking.^{21,23}

The solvation contribution due to electronic degrees of freedom of the solvent is much less discussed. It is related to the electronic polarizability of the solvent, as described by its refractive index at optical frequencies, and is then associated to fast degrees of freedom, that lead to a quasi-instantaneous adjustment of the electronic cloud of the solvent during an electronic transition of the solute. The narrow variability of the refractive index of common solvents hinders the experimental assessment of this solvation contribution and allowed to im-

explicitly account for fast solvation effects in ESMs via a renormalization of the model parameters, extracted from experiment.²⁹ However, fast solvation effects must be properly understood and explicitly accounted for in order to reliably parametrize ESMs against quantum-chemical calculations in gas-phase, or to address spectral properties of dyes in condensed media and, more generally, in media showing significantly different polarizabilities.

In a recent paper,³⁰ the role of fast solvation on spectral properties of organic molecules was addressed underlying how current approaches to environmental effects, as implemented in continuum solvation models^{31–35} as well as in mixed QM-MM approaches integrating quantum mechanical models for the molecular species and molecular mechanics models for the medium,³⁶ fail to properly address the phenomenon. Here we extend the discussion to several families of CT dyes, exploiting ESMs as a simple and effective tool to obtain a reliable interpretative scheme for solvation effects in these systems. Specifically, we will discuss how optical spectra of CT dyes are affected by the local environment, also addressing the role of solvation in driving symmetry breaking in quadrupolar and octupolar dyes.

II. THE MODEL

We consider three different families of dyes, dipolar, quadrupolar and octupolar systems, whose main resonating structures are depicted in Fig. 1. The electronic basis set is defined in all systems by the neutral structure $|N\rangle$, and either 1, 2 or 3 zwitterionic structures $|Z_i\rangle$ for dipolar, quadrupolar and octupolar systems, respectively. We consider perfectly symmetric quadrupolar and octupolar dyes. Accordingly, for each dye all zwitterionic structures are equivalent with energy $2z$ measured with respect to the $|N\rangle$ state, and are mixed to $|N\rangle$ by the same matrix element $-\tau$. The electronic Hamiltonian reads:

$$H_{el} = 2z\hat{\rho} - \tau \sum_{i=1}^n |Z_i\rangle \langle N| \quad (1)$$

where i runs over the n molecular branches ($n = 1$ for dipolar, $n = 2$ for quadrupolar and $n = 3$ for octupolar dyes) and $\hat{\rho} = \sum_{i=1}^n |Z_i\rangle \langle Z_i|$ is the ionicity operator measuring the cumulative weight of zwitterionic structures.

The dipole moment operator is defined on the diabatic basis, only accounting for its main contribution, i.e. assigning a sizable dipole of modulus μ_0 to each zwitterionic $D^+ - A^-$ branch. In the reference frame in Fig. 1, the dipole moment operator for the different structures reads:

$$\begin{aligned} \hat{\mu}_x &= \mu_0 \hat{\rho} & \hat{\mu}_y &= 0 & \hat{\mu}_z &= 0 & \text{dipolar} \\ \hat{\mu}_x &= \mu_0 \hat{\delta} & \hat{\mu}_y &= 0 & \hat{\mu}_z &= 0 & \text{quadrupolar} \\ \hat{\mu}_x &= \mu_0 \hat{\delta}_x & \hat{\mu}_y &= \mu_0 \hat{\delta}_y & \hat{\mu}_z &= 0 & \text{octupolar} \end{aligned} \quad (2)$$

where for the quadrupolar dye we have introduced the auxiliary operator

$$\hat{\delta} = |Z_1\rangle \langle Z_1| - |Z_2\rangle \langle Z_2| \quad (3)$$

and two auxiliary operators are needed for the octupolar dye:

$$\begin{aligned} \hat{\delta}_x &= \frac{\sqrt{3}}{2} (|Z_2\rangle \langle Z_2| - |Z_3\rangle \langle Z_3|) \\ \hat{\delta}_y &= -|Z_1\rangle \langle Z_1| + \frac{1}{2} (|Z_2\rangle \langle Z_2| + |Z_3\rangle \langle Z_3|) \end{aligned} \quad (4)$$

To account for the variation of the molecular geometry upon CT, an effective coordinate is introduced, q_i (p_i is the conjugated momentum) for each molecular arm. Assuming a harmonic potential with the same curvature for all basis states (linear electron-vibration coupling), the vibrational Hamiltonian reads:

$$H_{mol} = H_{el} - \sqrt{2\epsilon_v\omega_v} \sum_{i=1}^n q_i |Z_i\rangle \langle Z_i| + \frac{1}{2} \sum_{i=1}^n (\omega_v^2 q_i^2 + p_i^2) \quad (5)$$

where ω_v is the vibrational frequency and ϵ_v is the vibrational relaxation energy associated with the CT along each molecular arm.

For the sake of clarity, when dealing with the interaction between the dye and the surrounding medium we will use the term solute and solvent to refer to the dye and the medium, respectively, irrespective of their specific nature. In the simplest model, the solvent is described as a continuum elastic dielectric medium that is perturbed by the solute, described as a point dipole. The solvent then generates at the solute location an electric field (the reaction field) proportional to the solute dipole. The solute is in turn affected by the reaction field, leading to a self-consistent problem.^{19,28,37} The solvent reacts on two different time-scales: the electronic solvent response, with typical frequencies in the UV, is faster than the solute degrees of freedom. On the opposite, the orientational motion of polar solvent molecules is much slower than the electronic and vibrational degrees of freedom of the solute. Accordingly, the reaction field \vec{F}_R is separated into an electronic (subscript *el*) and an orientational (subscript *or*) contribution, both proportional to the solute dipole moment:

$$\vec{F}_R = \vec{F}_{el} + \vec{F}_{or} = r_{el} \langle \vec{\mu} \rangle + r_{or} \langle \vec{\mu} \rangle \quad (6)$$

The $r_{el/or}$ prefactors depend on the dielectric properties of the medium. Explicit expressions have been derived relating these quantities to the medium refractive index, dielectric constant and the shape and size of the cavity occupied by the solute.^{28,37} Irrespective of the specific model, the orientational component of the solvation field is sizable only for polar solvents, so that $r_{or} \sim 0$ in non-polar media.

The different timescales of the two components of the reaction field call for different approximation schemes.

Specifically, the adiabatic approximation can safely be applied to slow solvation, while fast solvation can be dealt with in the antiadiabatic approximation,³⁸ as discussed in Ref. 30. Accordingly, the complete Hamiltonian, also accounting for the solute-solvent interaction, reads

$$H = H_{mol} + \left[\frac{F_{el}^2}{2r_{el}} + T_{el} - \hat{\mu} \cdot \vec{F}_{el} \right] + \left[\frac{F_{or}^2}{2r_{or}} - \hat{\mu} \cdot \vec{F}_{or} \right] \quad (7)$$

where the terms relevant to electronic and orientational solvation have been separated into square brackets. In both terms the quadratic contribution in the reaction field accounts for the potential energy (the energy required to create the field) in the harmonic approximation. The relevant force constant is fixed to $(r_{el/or})^{-1}$ upon imposing the equilibrium condition in Eq. 6.^{29,30} The kinetic energy relevant to polar solvation is neglected in the adiabatic approximation, while it is accounted for as T_{el} for the electronic component. Polar solvation has been extensively discussed in the framework of ESMs and will not be addressed here. We therefore only discuss the electronic (fast) contribution to solvation dropping the last term in the Hamiltonian in Eq. 7, setting $F_{or} = 0$, as relevant to non-polar solvents.

The effective frequency ω_{el} associated to the fast component of the reaction field accounts for the electronic excitation of the solvent, typically in the mid-far UV regions, at much higher frequencies than the transition frequencies of the solute, in the visible or near-UV region. Accordingly, we adopt an antiadiabatic approximation, setting $\omega_{el} \rightarrow \infty$,³⁰ to define the following renormalized solute Hamiltonian, implicitly accounting for fast solvation:³⁰

$$H_{AA} = H_{mol} - \frac{r_{el}}{2} \hat{\mu}^2 \quad (8)$$

Fast solvation then introduces a two-electron term in the electronic Hamiltonian, that however, in ESM acquires a very simple form with a clear physical meaning. Indeed for all CT dyes discussed here, with dipolar, quadrupolar or octupolar structure, one finds $\hat{\mu}^2 = \mu_0^2 \hat{\rho}$, so that

$$H_{AA} = H_{mol} - \epsilon_{el} \hat{\rho} \quad (9)$$

where $\epsilon_{el} = \mu_0^2 r_{el} / 2$ measures the amount of energy gained by the system in a zwitterionic state due the relaxation of the electronic clouds of the solvent molecule. In other terms, when going from gas phase to solution, the energy $2z$ required to separate a charge along a molecular arm is reduced by the solvent relaxation energy related to fast solvation, so that $z \rightarrow z - \epsilon_{el} / 2$.

The above equations are fairly general and do not depend on the details of solvation model. Relating ϵ_{el} to the solvent properties and specifically to the solvent refractive index, requires however a specific description of the solute-solvent system. A widely adopted approach assumes that the solute occupies a spherical cavity in the solvent, with radius a .^{28,37} In this hypothesis

$$r_{el} = \frac{2}{4\pi\epsilon_0 a^3} \frac{\eta^2 - 1}{2\eta^2 + 1} \quad (10)$$

where η is the solvent refractive index at optical frequencies. We will use this approximate relation to estimate a reasonable variability range for ϵ_{el} .

In the following, we will present selected results obtained for the three families of dyes in Fig. 1, to discuss the effects of the medium polarizability on molecular properties. Relevant results will be compared with results obtained adopting the adiabatic approximation to describe fast solvation. In this approximation, the kinetic energy associated with the electronic degrees of freedom of the solvent, T_{el} in Eq. 7, is neglected and an effective Hamiltonian is defined for each electronic state of the solute, fixing \vec{F}_{el} to its equilibrium value relevant the specific state of interest. Due to the fast dynamics involved in the solvent electronic polarization, the adiabatic approximation is clearly not suitable to describe fast solvation.³⁰ However, current implementations of continuum solvation models in quantum chemical codes all rely in the adiabatic approximation for both the orientational and electronic components of solvation field,³⁹⁻⁴¹ and the same approximation is also adopted in current application of QM-MM models.³⁶ It is therefore important to stress the limits of this widely adopted, even if not explicitly acknowledged, approximation.

III. RESULTS AND DISCUSSION

A. Polar dyes

Neglecting electron-vibration coupling ($\epsilon_v = 0$ in Eq. 5), the molecular properties of polar D- π -A dyes only depend on the z/τ ratio. In the following we use units such that $\hbar = 1$ and set τ as the energy unit. The actual τ value for most CT dyes is of the order of 1 eV,²⁶ even if for dyes of interest for thermally delayed fluorescence applications,^{3,42,43} typical τ are one order of magnitude smaller. All properties of interest can be expressed as a function of ρ : the transition dipole moment is $\mu_{CT} = \mu_0 \sqrt{\rho(1-\rho)}$, showing a maximum at $\rho = 0.5$, and the transition frequency is $\omega_{CT} = \tau / \sqrt{\rho(1-\rho)}$, showing a minimum at $\rho = 0.5$. The permanent dipole moment is $\mu_G = \mu_0 \rho$ and $\mu_E = \mu_0(1-\rho)$ in the ground and excited state, respectively, so that the mesomeric dipole moment $\mu_E - \mu_G = \mu_0(1-2\rho)$ is positive for mostly neutral dyes ($\rho < 0.5$) and negative for mostly zwitterionic dyes ($\rho > 0.5$). Accordingly, mostly neutral dyes show normal solvatochromic behavior (the absorption band redshifts upon increasing solvent polarity) while mostly zwitterionic dyes show inverse solvatochromism (the absorption band blueshifts upon increasing solvent polarity), so that a simple spectroscopic data allow to discriminate between the two classes of polar dyes.

Fig. 2 collects results for a mostly neutral dye ($z = 0.75$, corresponding to $\rho_{gas} = 0.2$) and a mostly zwitterionic dye ($z = -0.75$, $\rho_{gas} = 0.8$). Analytical results for the purely electronic model ($\epsilon_v = 0$) in panels a-c and f-h show the evolution of the molecular properties when ϵ_{el}

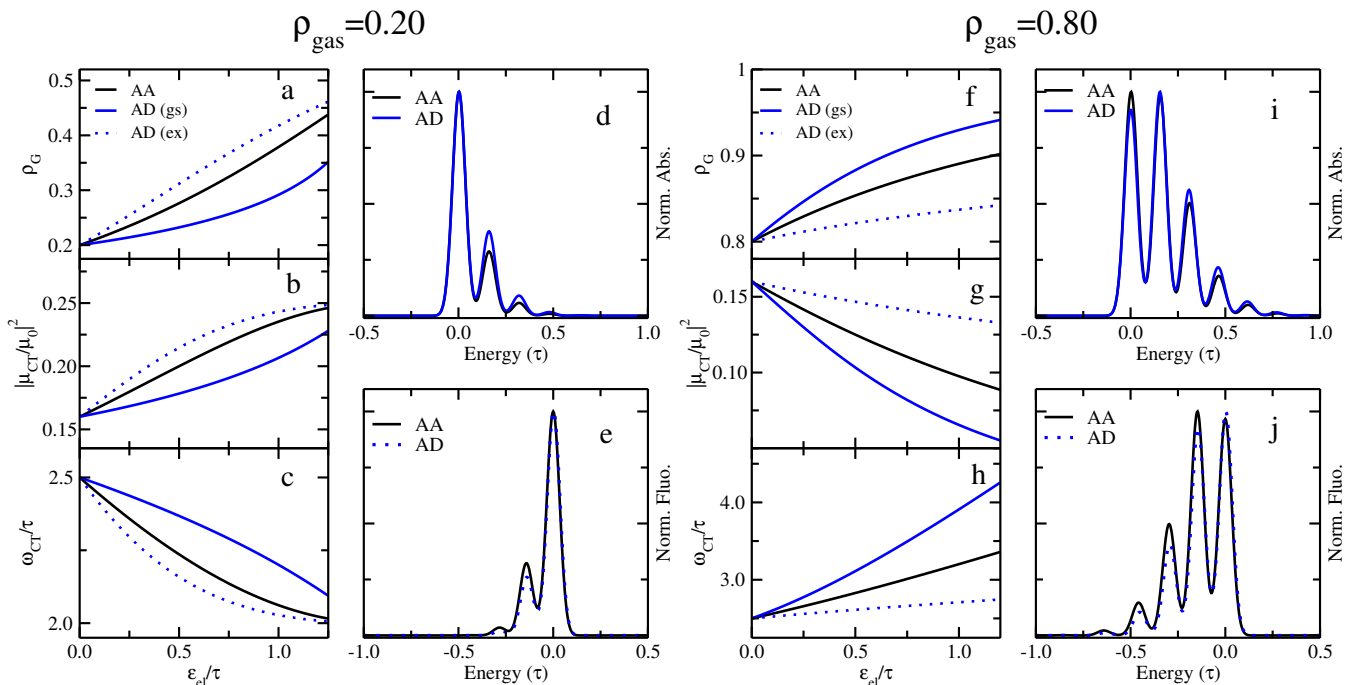


FIG. 2. Fast solvation effects on the properties of polar chromophores with $\rho_{gas} = 0.2$ (left side) or $\rho_{gas} = 0.8$ (right side). On each side, right panels show properties (ground-state ionicity, transition dipole moment, transition frequency) as a function of ϵ_{el} for a system with $\epsilon_v = 0$. The right panels show vibronic bandshapes calculated for a system with $\epsilon_v = 0.3$ and $\epsilon_{el} = 0.32$. Antiadiabatic (AA) results: black lines; Adiabatic (AD) results with F_{el} equilibrated with the ground state (full blue lines) or with the optically-allowed excited state (dotted blue lines).

increases from 0, as relevant to the gas phase, to larger values, typical of organic media. In all cases, the ionicity ρ increases with ϵ_{el} , as a result of the stabilization of charge separated states by the electronic polarizability of the environment. Adiabatic results (blue lines in Fig. 2) show quantitative and sometimes sizable deviations from the antiadiabatic results (black curves), but the most clear failure of the adiabatic approach is recognized in having two different sets of results, corresponding to the two different adiabatic Hamiltonians obtained upon fixing the reaction field to the equilibrium value for the ground state (blue continuous lines) or for the excited state (blue dotted lines). This is clearly unphysical, since the electronic clouds of solvent molecules readjust quickly (instantaneously in the antiadiabatic limit) to the charge reorganization in the solute. In any case, taking adiabatic results at face value, one should use the adiabatic Hamiltonian with F_{el} equilibrated to the ground state or to the excited state to simulate absorption or fluorescence processes, respectively. This leads to a spurious red-shift of the fluorescence band with respect to the absorption band. To get rid of this spurious Stokes-shift, two different approaches are currently implemented in quantum chemical packages. In the first approach, first order perturbation theory is used to calculate the energy corrections due to solvation, without the need to diagonalize two different Hamiltonians.^{32,34} In the second approach the transition energy (coincident for absorption

and fluorescence) is defined as the difference between the energy of the excited state, calculated diagonalizing the adiabatic Hamiltonian with F_{el} equilibrated to the excited state, and the energy of the ground state, calculated diagonalizing the adiabatic Hamiltonian with F_{el} equilibrated to the ground-state.⁴⁴ This strategy is however untenable on physical grounds, as it defines electronic transitions between states obtained upon diagonalizing two different Hamiltonians. The inconsistency of the approach, leading to undefined transition dipole moments, most clearly points to the fundamental failure of the adiabatic approach to fast solvation.

To address vibronic bandshapes we account for electron-vibration coupling in a non-adiabatic calculation. Specifically, we solve the molecular Hamiltonian in Eq. 5 (modified as in Eq. 8 to account for fast solvation in the antiadiabatic limit, or accounting for the static corrections due to the equilibrated F_{el} in the adiabatic limit) by writing the corresponding matrix on the basis defined as the direct product of the electronic basis states times the eigenstates of the harmonic oscillator(s) in the last term of equation 5. Of course the vibrational basis is truncated to a large enough number of vibrational states as to obtain convergence. Once the molecular Hamiltonian is diagonalized, the absorption and fluorescence spectra are calculated from the transition energies and transition dipole moments assigning each vibronic transition a Gaussian lineshape with fixed linewidth (in this

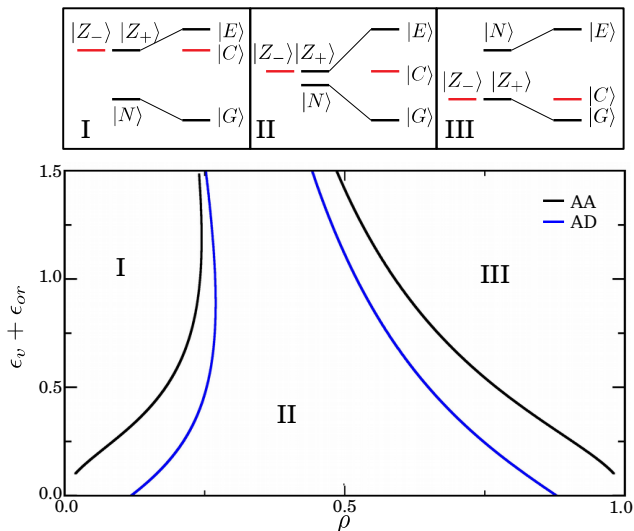


FIG. 3. Top panels: sketch of the essential states of class I, II and III quadrupolar dyes. Bottom panel: phase diagram for quadrupolar dyes. The black lines show antiadiabatic (AA) results, the blue lines show adiabatic (AD) results for $\epsilon_{el} = 0.3$.

work it is set to 0.04).⁴⁵ In the antiadiabatic approach to fast solvation the eigenstates obtained upon diagonalization of a single effective Hamiltonian enter the calculation of both absorption and fluorescence spectra. On the opposite, in the adiabatic approach to fast solvation two different Hamiltonians with F_{el} equilibrated either to the ground or to the excited state are used for the calculation of absorption and fluorescence spectra, respectively. In Fig. 2, the rightmost panels relevant to each dye show an example of vibronic bandshapes calculated for absorption and emission spectra setting $\epsilon_v = 0.3$. Since we are interested in comparing bandshapes, all normalized spectra are translated to set the origin of the energy axis at the 0-0 transition energy. Calculated absorption and fluorescence bandshapes in the adiabatic approximation are marginally different from antiadiabatic results.

B. Quadrupolar chromophores

To address the electronic problem of quadrupolar dyes we exploit symmetry, combining the two degenerate basis states $|Z_1\rangle$ and $|Z_2\rangle$ as $|Z_{\pm}\rangle = (|Z_1\rangle \pm |Z_2\rangle)/\sqrt{2}$. The mixing between $|Z_{+}\rangle$ and $|N\rangle$ gives the ground state $|G\rangle$ and an excited state $|E\rangle$. The excited state $|E\rangle$ cannot be reached upon one-photon absorption and is located at higher energy than the optically active state $|C\rangle = |Z_{-}\rangle$. The mixing between $|N\rangle$ and $|Z_{+}\rangle$ only depend on the z/τ ratio.²¹ As sketched in the top panels of Fig. 3, systems with large mixing ($\rho \sim 0.5$) are characterized by large transition energies (class II dyes), while systems with small mixing ($\rho \rightarrow 0$ or 1 class I or III dyes, res-

pectively) show a pair of quasi-degenerate eigenstates, signalling a conditional instability.²¹

Studying the problem for the isolated molecule in the gas phase (Eq. 5) we can collect valuable information about the tendency of the dye towards symmetry breaking, adopting an adiabatic approximation to treat molecular vibrations. Along these lines, the potential energy surfaces (PES) for the ground and excited states can be drawn and analytical results may be obtained for the phase diagram of quadrupolar dyes (bottom panel of Fig. 3). In the (ϵ_v, ρ) plane the black curves mark the boundaries between the three different classes: for class I dyes the PES associated to the first excited state shows a double minimum, suggesting the tendency to symmetry breaking for this state. Class II dyes are characterized by well-behaved PES for all three states that are therefore not prone to symmetry-breaking. Finally class III dyes are characterized by a bistable ground state. It is important to underline at this stage that symmetry breaking cannot be observed in an isolated molecule.⁴⁶ The double minimum in the excited or ground state of systems in class I or III, respectively, does not necessarily imply a symmetry breaking phenomenon, since any finite-size system will always oscillate between the two minima recovering the full symmetry of the system in a sort of dynamical Jahn-Teller effect.⁴⁷ Of course a genuine symmetry breaking may be observed if the dye is dissolved in a polar solvent. Polar solvation, corresponding to an extremely slow motion, can be described accurately in the adiabatic approximation, and the relevant relaxation energy, $\epsilon_{or} = \mu_0^2 r_{el}/2$, enters the picture summing up to ϵ_v in the phase diagram in Fig. 3, thus widening the region where either the ground or excited state instability occurs.²¹ Even more importantly, the slow motion of polar solvation basically freezes the system in one of the minima not allowing tunneling in any time of relevance to optical spectroscopy. Symmetry breaking driven by polar solvation in the excited state of class I polar dyes quite naturally explains the large positive solvatochromism observed in fluorescence spectra of these systems,^{21,24} while the ground-state symmetry breaking in class III dyes is the key to understand the anomalous absorption solvatochromism observed in long cyanine dyes, in spite of their nominally symmetric structure.^{23,48}

Accounting for fast solvation does not alter the picture. Indeed in the antiadiabatic approximation, the electronic polarizability of the solvent lowers the energy gap $2z$, as discussed in Section II, leading to an increase of ρ . However, the phase diagram in Fig. 3 still applies: the black lines separating the different regions in the phase diagram are not affected by the variation of the medium refractive index. Instead, if the adiabatic approximation is incorrectly enforced to describe fast solvation, the relevant relaxation energy ϵ_{el} would enter the picture much as in the case of polar solvation, hence summing up to ϵ_v in Fig. 3 favoring symmetry breaking. In other terms, as illustrated in the phase diagram in Fig. 3 for the specific case $\epsilon_{el} = 0.3$ (blue lines), the boundaries between the

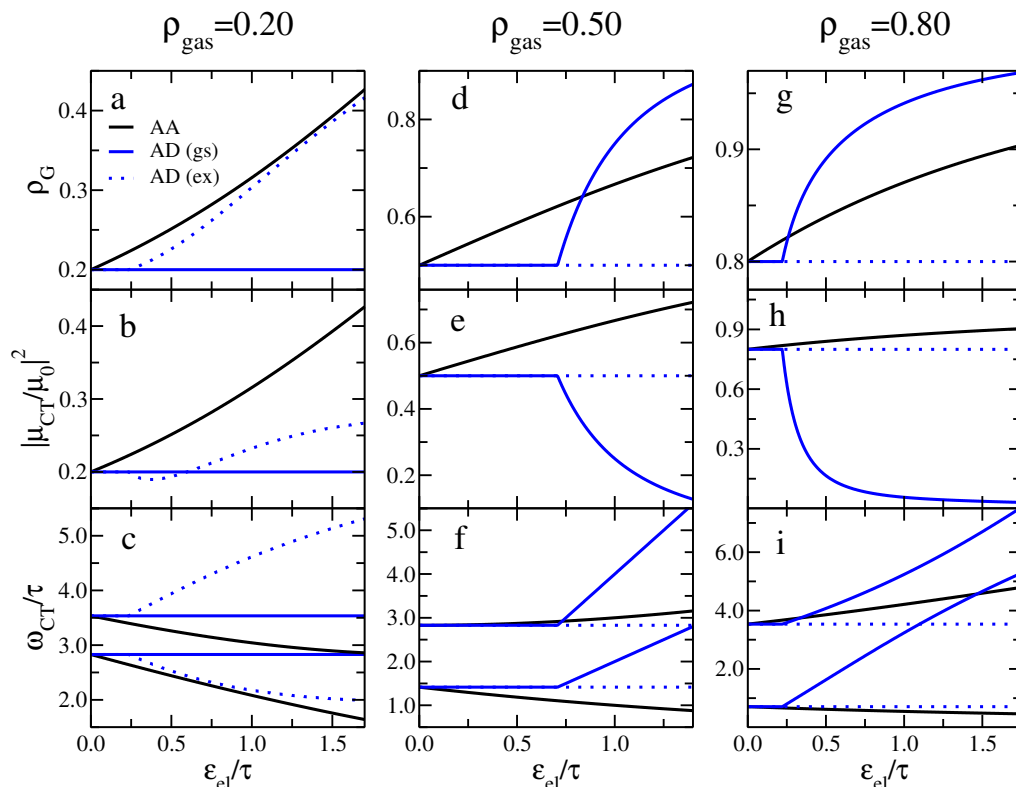


FIG. 4. Fast solvation effects on the properties (ground-state ionicity, transition dipole moment, transition frequency) of quadrupolar dyes belonging to different classes and with $\epsilon_v = 0$. Two transition energies are shown corresponding to the C and E states (lower and higher transition energy, respectively). The transition dipole relevant to the transition from the ground to the E state vanishes and is not shown. Antiadiabatic (AA) results: black lines; Adiabatic (AD) results with F_{el} equilibrated with the ground state (full blue lines) or with the optically-allowed excited state (dotted blue lines). The abrupt changes observed in adiabatic results mark the occurrence of symmetry breaking.

different regions in the phase diagram would be downshifted by ϵ_{el} , artificially widening the instability regions associated with class I and class III dyes.

Fig. 4 shows analytical results for the electronic model ($\epsilon_v = \epsilon_{or} = 0$) relevant to three quadrupolar systems with z adjusted as to have $\rho_{gas} = 0.2$, 0.5 and 0.8 , as representative of class I, II and III dyes, respectively. In all cases, the antiadiabatic results (black lines) predict an increase of ρ with increasing the medium polarizability. This always implies an increase of the transition dipole moment μ_{CT} for the allowed $G \rightarrow C$ transition. For the class I system ($\rho_{gas} = 0.2$) the two transition frequencies ($G \rightarrow C$ and $G \rightarrow E$) decrease considerably with the medium refractive index, while the effects are less pronounced in the other two systems, with the lowest (highest) transition decreasing (increasing) in energy with ϵ_{el} .

Enforcing the adiabatic approximation for fast solvation leads to different Hamiltonians, depending on the reference state selected to equilibrate the reaction field. Continuous and dotted blue lines in Fig. 4 refer to adiabatic results obtained fixing F_{el} to the equilibrium value relevant to the ground state or to the optically-allowed (C) excited state, respectively. Since the ground-state

dipole moment vanishes as long as the ground state symmetry is conserved, adiabatic results obtained for F_{el} equilibrated to the ground state do not vary at all with ϵ_{el} as long as the ground-state symmetry is preserved. This is the case for the quadrupolar dye with $\rho_{gas} = 0.2$ (left panels), where no variation of either ρ_G or μ_{CT} or ω_{CT} is obtained in the ground-state adiabatic approximation (full blue lines) when ϵ_{el} is increased. On the other hand, adiabatic results obtained for F_{el} equilibrated to the optically-allowed excited state do not vary at all with ϵ_{el} as long as the excited-state symmetry is preserved. This is the case of the quadrupolar dye with $\rho_{gas} = 0.8$ (right panels), where no variation of either ρ_G or μ_{CT} or ω_{CT} is obtained in the excited-state adiabatic approximation (dotted blue lines) when ϵ_{el} is increased. The adiabatic results contrast sharply with antiadiabatic results that instead properly account for the effect of the solvent polarizability on molecular properties.

However, the most striking failure of the adiabatic approximation to fast solvation in quadrupolar systems is the prediction of spurious symmetry-breaking phenomena. The class II system in the middle panels of Fig. 3 ($\rho_{gas} = 0.5$) is a paradigmatic example: if electronic solvation is properly described in the antiadiabatic approx-

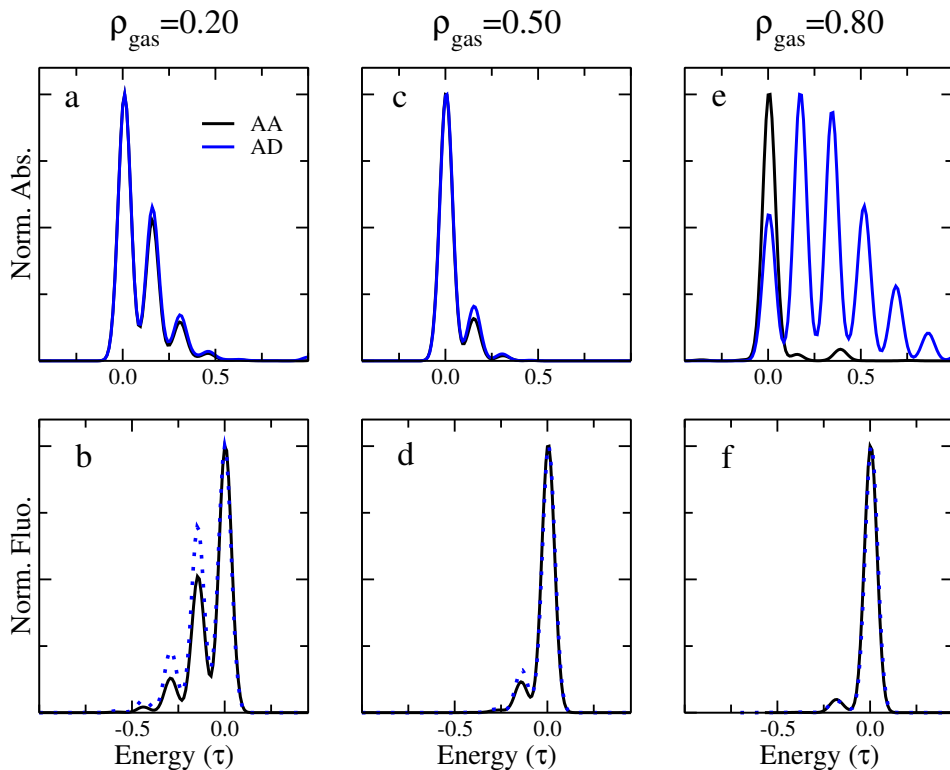


FIG. 5. Vibronic absorption (top) and fluorescence (bottom) spectra for quadrupolar dyes of different classes, for $\epsilon_v = 0.3$ and $\epsilon_{el} = 0.32\tau$. Black lines: antiadiabatic results; Blue lines: adiabatic results.

imation, the system is not prone to symmetry breaking, but, if a ground state adiabatic approach is enforced, the ground state undergoes symmetry breaking at $\epsilon_{el} \approx 0.75$, as shown by the abrupt variation of the molecular properties (full blue lines). At the same time, symmetry is preserved in the excited state, so that in the adiabatic approximation, when F_{el} is equilibrated to the C state, ϵ_{el} does not affect molecular properties (dotted blue lines). For the system with $\rho_{gas} = 0.8$, the ground-state adiabatic approximation predicts symmetry breaking in the ground state for $\epsilon_{el} > 0.25$, while symmetry is preserved in the C state. For the system with $\rho_{gas} = 0.2$, the excited-state adiabatic approximation predicts symmetry breaking in the C state for $\epsilon_{el} > 0.30$, while symmetry is preserved in the ground state.

Vibronic bandshapes are shown in Fig. 5 for the same three representative systems, but fixing $\epsilon_v = 0.3$ and $\epsilon_{el} = 0.32$. Marginal differences between the antiadiabatic and adiabatic results are found as long as symmetry is conserved in the adiabatic calculation, while sizable deviations are of course observed for emission spectra of class I dyes and huge deviations for absorption spectra of class III dyes, due to spurious symmetry-breaking effects.

C. Octupolar chromophores

The threefold rotation axis in octupolar chromophores implies the presence of doubly degenerate states, which leads to instability in either the ground or excited state, precluding the presence of class II dyes, as shown in the phase diagram in the bottom panel of Fig. 6.²⁷ As in the case of quadrupolar chromophores, the phase diagram, plotted against the ground-state ionicity, is independent of ϵ_{el} in the correct antiadiabatic limit (black line). In the adiabatic approximation instead the boundary is lowered along the ordinate by ϵ_{el} (blue line).

The left panels of Fig. 6 show the molecular properties calculated for an octupolar dye with $\rho_{gas} = 0.2$ (to the best of our knowledge there are no examples of octupolar dyes of class III). The antiadiabatic calculation predicts, as expected, an increasing contribution of zwitterionic states into the ground state (increasing ρ) when ϵ_{el} is increased. Concomitantly, the transition dipole moment towards the optically-allowed state, corresponding to a doubly degenerate state, increases while the excitation energy towards either the lowest-energy (allowed) or the highest-energy (forbidden) excited states decreases. The system stays stable, preserving its symmetry, as long as slow degrees of freedom do not enter into play. The adiabatic calculation instead predicts no effect of the medium polarizability when F_{el} is equilibrated to the ground state. On the opposite, when the reaction field is

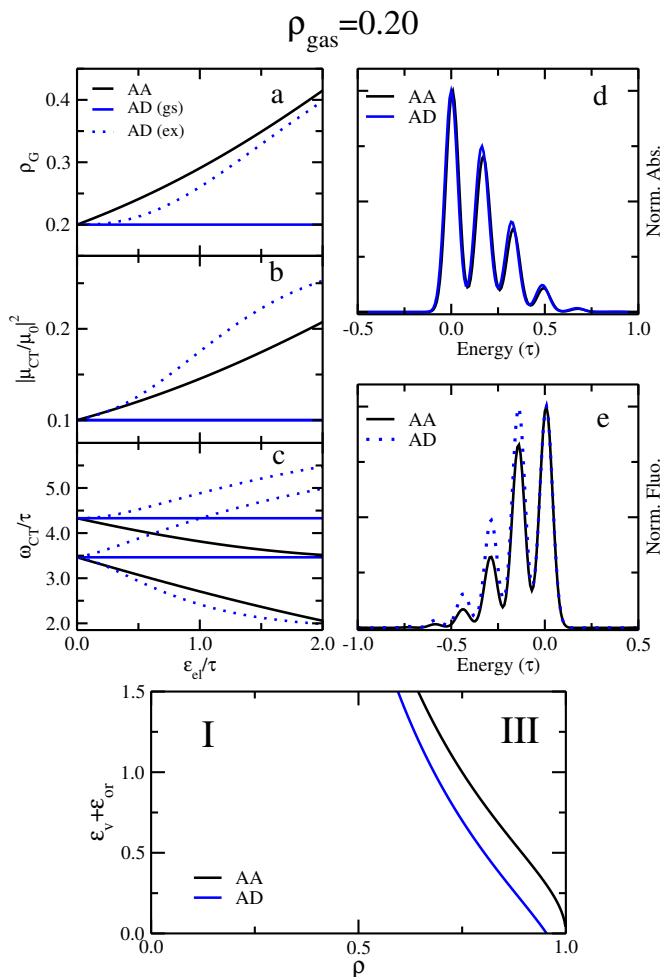


FIG. 6. Top panels: fast solvation effects on an octupolar chromophore with $\rho_{gas} = 0.20$. Black lines show antiadiabatic (AA) results; blue lines show adiabatic (AD) results with F_{el} equilibrated with the ground state (continuous lines) or with the optically-allowed excited state (dotted lines). Panels (a-c) show the electronic properties (ground-state ionicity, transition dipole moment, transition frequencies) as a function of ϵ_{el} for a system with $\epsilon_v = 0$. Panels (d) and (e) show vibronic absorption and fluorescence spectra, respectively, calculated for $\epsilon_{el} = 0.32$ and $\epsilon_v = 0.3$. Bottom panel: phase diagram ($\epsilon_{el} = 0.3$ for the adiabatic, AD, result).

equilibrated to the lowest excited state, clear signatures of a spurious symmetry breaking appear. As for vibronic bandshapes, results in Fig. 6(d) and (e) for the dye with $\rho_{gas} = 0.2$, $\epsilon_v = 0.3$ and $\epsilon_{el} = 0.32$ show marginal differences between spectra calculated in the adiabatic vs the antiadiabatic approximation.

IV. CONCLUSIONS

Solvation is a complex phenomenon involving several degrees of freedom characterized by different timescales. In particular, a slow component of solvation is driven

by the orientational motion of polar solvent molecules around the solute, and is only relevant to polar solvents. Another component is instead always present, irrespective of the solvent polarity, and is related to the solvent electronic polarizability, as measured by the solvent refractive index. This corresponds to a fast motion, since the electronic excitations of the solvent typically fall in the mid/far-UV region, i.e. at significantly higher frequencies than relevant degrees of freedom of organic dyes. While the slow component of solvation can be safely dealt with in the adiabatic approximation, the same approximation is not suitable to treat fast solvation, that can instead be treated in the antiadiabatic approximation.³⁰ Here we discussed spectroscopic effects of fast solvation with reference to ESMs for CT dyes of different families. In particular, we discussed how the medium polarizability affects optical spectra of dipolar, quadrupolar and octupolar dyes, comparing results obtained in the antiadiabatic approximation with those obtained in an adiabatic approach. This is not a trivial exercise since current implementations of solvation models and more generally all quantum-classical description of molecules in solution rely on an adiabatic treatment of fast solvation. Apart from quantitative deviations, the adiabatic approximation to fast solvation leads to spurious Stokes shifts (measuring the difference between the energy of the absorption and emission transitions) that are currently cured either limiting the treatment to a first order perturbation approach or accounting for a transition occurring between states obtained as eigenstates of two different Hamiltonians.

Moreover, in quadrupolar and octupolar dyes, applying the adiabatic approximation to fast solvation can drive symmetry breaking in systems where it cannot possibly occur. Specifically, genuine symmetry breaking can never occur in isolated (gas phase) molecular systems,⁴⁶ nor can it be induced by fast solvation. Only polar solvation, associated with an extremely slow, classical coordinate may drive a *bona fide* symmetry breaking in a molecular system. Symmetry breaking phenomena as often discussed in chemical literature⁴⁹⁻⁵² in the gas-phase or in non-polar solvents are actually an artifact associated with the adiabatic treatment of vibrational degrees of freedom and/or of fast solvation.

ACKNOWLEDGMENTS

This project received funding from the European Union Horizon 2020 research and innovation programme under Grant Agreement No. 812872 (TADFLife), and benefited from the equipment and support of the COMP-HUB Initiative, funded by the Departments of Excellence program of the Italian Ministry for Education, University and Research (MIUR, 2018-2022). We acknowledge the support from the HPC (High Performance Computing) facility of the University of Parma, Italy.

- * anna.painelli@unipr.it
- ¹ B. Kippelen and J.-L. Brdas, *Energy Environ. Sci.* **2**, 251 (2009).
 - ² A. P. Kulkarni, C. J. Tonzola, A. Babel, and S. A. Jenekhe, *Chemistry of Materials* **16**, 4556 (2004), <https://doi.org/10.1021/cm049473l>.
 - ³ M. Y. Wong and E. Zysman-Colman, *Advanced Materials* **29**, 1605444 (2017), <https://onlinelibrary.wiley.com/doi/pdf/10.1002/adma.201605444>.
 - ⁴ W. Prasad, *Nonlinear Optical* (John Wiley & Sons, 1991).
 - ⁵ *Molecular Nonlinear Optics* (Elsevier, 1994).
 - ⁶ F. Terenziani, C. Katan, E. Badaeva, S. Tretiak, and M. Blanchard-Desce, *Advanced Materials* **20**, 4641 (2008).
 - ⁷ G. S. He, L.-S. Tan, Q. Zheng, and P. N. Prasad, *Chemical Reviews* **108**, 1245 (2008).
 - ⁸ S. A. Kovalenko, J. L. Prez Lustres, N. P. Ernstring, and W. Rettig, *The Journal of Physical Chemistry A* **107**, 10228 (2003), <https://doi.org/10.1021/jp026802t>.
 - ⁹ E. Campioli, S. Sanyal, A. Marcelli, M. Di Donato, M. Blanchard-Desce, O. Mongin, A. Painelli, and F. Terenziani, *ChemPhysChem* **20**, 2860 (2019), <https://chemistry-europe.onlinelibrary.wiley.com/doi/pdf/10.1002/cphc.201900703>.
 - ¹⁰ F. Terenziani, G. D'Avino, and A. Painelli, *ChemPhysChem* **8**, 2433 (2007), <https://chemistry-europe.onlinelibrary.wiley.com/doi/pdf/10.1002/cphc.200700368>.
 - ¹¹ F. Terenziani and A. Painelli, *Phys. Rev. B* **68**, 165405 (2003).
 - ¹² A. Painelli and F. Terenziani, *Journal of the American Chemical Society* **125**, 5624 (2003), pMID: 12733888, <https://doi.org/10.1021/ja034155t>.
 - ¹³ S. Sanyal, A. Painelli, S. K. Pati, F. Terenziani, and C. Sissa, *Phys. Chem. Chem. Phys.* **18**, 28198 (2016).
 - ¹⁴ S. Sanyal, C. Sissa, F. Terenziani, S. K. Pati, and A. Painelli, *Phys. Chem. Chem. Phys.* **19**, 24979 (2017).
 - ¹⁵ B. Bardi, C. Dall'Agnese, K. I. Moineau-Chane Ching, A. Painelli, and F. Terenziani, *The Journal of Physical Chemistry C* **121**, 17466 (2017), <https://doi.org/10.1021/acs.jpcc.7b04647>.
 - ¹⁶ B. Bardi, C. Dall'Agnese, M. Tass, S. Ladeira, A. Painelli, K. I. Moineau-Chane-Ching, and F. Terenziani, *ChemPhotoChem* **2**, 1027 (2018), <https://chemistry-europe.onlinelibrary.wiley.com/doi/pdf/10.1002/cptc.201800148>.
 - ¹⁷ C. Zhong, D. Bialas, and F. C. Spano, *The Journal of Physical Chemistry C* **124**, 2146 (2020), <https://doi.org/10.1021/acs.jpcc.9b09368>.
 - ¹⁸ C. Zheng, C. Zhong, C. J. Collison, and F. C. Spano, *The Journal of Physical Chemistry C* **123**, 3203 (2019), <https://doi.org/10.1021/acs.jpcc.8b11416>.
 - ¹⁹ W. Liptay, *Angewandte Chemie International Edition in English* **8**, 177 (1969), <https://onlinelibrary.wiley.com/doi/pdf/10.1002/anie.196901777>.
 - ²⁰ C. Reichardt, *Chemical Reviews* **94**, 2319 (1994), <https://doi.org/10.1021/cr00032a005>.
 - ²¹ F. Terenziani, A. Painelli, C. Katan, M. Charlot, and M. Blanchard-Desce, *Journal of the American Chemical Society* **128**, 15742 (2006), pMID: 17147384, <https://doi.org/10.1021/ja064521j>.
 - ²² J. Campo, A. Painelli, F. Terenziani, T. Van Regemorter, D. Beljonne, E. Goovaerts, and W. Wenseleers, *Journal of the American Chemical Society* **132**, 16467 (2010), pMID: 21033705, <https://doi.org/10.1021/ja105600t>.
 - ²³ F. Terenziani, O. V. Przhonska, S. Webster, L. A. Padilha, Y. L. Slominsky, I. G. Davydenko, A. O. Gerasov, Y. P. Kovtun, M. P. Shandura, A. D. Kachkovski, D. J. Hagan, E. W. Van Stryland, and A. Painelli, *The Journal of Physical Chemistry Letters* **1**, 1800 (2010), <https://doi.org/10.1021/jz100430x>.
 - ²⁴ H. Hu, O. V. Przhonska, F. Terenziani, A. Painelli, D. Fishman, T. R. Ensley, M. Reichert, S. Webster, J. L. Bricks, A. D. Kachkovski, D. J. Hagan, and E. W. Van Stryland, *Phys. Chem. Chem. Phys.* **15**, 7666 (2013).
 - ²⁵ A. Painelli and F. Terenziani, *Chemical Physics Letters* **312**, 211 (1999).
 - ²⁶ B. Boldrini, E. Cavalli, A. Painelli, and F. Terenziani, *J. Phys. Chem. A* **106**, 6286 (2002).
 - ²⁷ F. Terenziani, C. Sissa, and A. Painelli, *The Journal of Physical Chemistry B* **112**, 5079 (2008), pMID: 18376886, <https://doi.org/10.1021/jp710241g>.
 - ²⁸ S. Di Bella, T. J. Marks, and M. A. Ratner, *J. Am. Chem. Soc.* **116**, 4440 (1994).
 - ²⁹ A. Painelli, *Chem. Phys.* **245**, 185 (1999).
 - ³⁰ D. K. A. Phan Huu, R. Dhali, C. Pieroni, F. Di Maiolo, C. Sissa, F. Terenziani, and A. Painelli, *Phys. Rev. Lett.* **124**, 107401 (2020).
 - ³¹ J. Tomasi, B. Mennucci, and R. Cammi, *Chem. Rev.* **105**, 2999 (2005).
 - ³² A. V. Marenich, C. J. Cramer, D. G. Truhlar, C. A. Guido, B. Mennucci, G. Scalmani, and M. J. Frisch, *Chem. Sci.* **2**, 2143 (2011).
 - ³³ B. Lunkenheimer and Köhn, *J. Chem. Theory Comput.* **9**, 977 (2013).
 - ³⁴ C. A. Guido and S. Caprasecca, *Int. J. Quantum Chem.* **119**, e25711 (2019).
 - ³⁵ J. Li, G. D'Avino, I. Duchemin, D. Beljonne, and X. Blase, *Phys. Rev. B* **97**, 035108 (2018).
 - ³⁶ T. Vreven and K. Morokuma (Elsevier, 2006) pp. 35 – 51.
 - ³⁷ E. G. McRae, *J. Phys. Chem.* **61**, 1128 (1957).
 - ³⁸ D. Feinberg, S. Ciuchi, and F. De Pasquale, *Int. J. Modern Phys. B* **4**, 1317 (1990).
 - ³⁹ R. Cammi, S. Corni, B. Mennucci, and J. Tomasi, *The Journal of Chemical Physics* **122**, 104513 (2005), <https://doi.org/10.1063/1.1867373>.
 - ⁴⁰ R. Improta, V. Barone, G. Scalmani, and M. J. Frisch, *The Journal of Chemical Physics* **125**, 054103 (2006), <https://doi.org/10.1063/1.2222364>.
 - ⁴¹ C. A. Guido and S. Caprasecca, *International Journal of Quantum Chemistry* **119**, e25711 (2019), <https://onlinelibrary.wiley.com/doi/pdf/10.1002/qua.25711>.
 - ⁴² H. Nakanotani, T. Higuchi, T. Furukawa, K. Masui, K. Morimoto, M. Numata, H. Tanaka, Y. Sagara, T. Yasuda, and C. Adachi, *Nature Communications* **5**, 4061 (2014).
 - ⁴³ P. Pander, R. Motyka, P. Zassowski, M. K. Etherington, D. Varsano, T. J. da Silva, M. J. Caldas, P. Data, and A. P. Monkman, *The Journal of Physical Chemistry C* **122**, 23934 (2018), <https://doi.org/10.1021/acs.jpcc.8b07610>.
 - ⁴⁴ R. Improta, V. Barone, G. Scalmani, and M. J. Frisch, *J. Chem. Phys.* **125**, 054103 (2006).
 - ⁴⁵ C. Sissa, V. Calabrese, M. Cavazzini, L. Grisanti, F. Terenziani, S. Quici, and A. Painelli, *Chemistry - A European Journal* **19**, 924 (2012).
 - ⁴⁶ P. W. Anderson, *Basic Notions of Condensed Matter*

- Physics* (CRC Press, Boca Raton, FL, 1996).
- ⁴⁷ C. Sissa, F. Delchiaro, F. Di Maiolo, F. Terenziani, and A. Painelli, *The Journal of Chemical Physics* **141**, 164317 (2014), <https://doi.org/10.1063/1.4898710>.
- ⁴⁸ C. Sissa, P. M. Jahani, Z. G. Soos, and A. Painelli, *ChemPhysChem* **13**, 2795 (2012), <https://chemistry-europe.onlinelibrary.wiley.com/doi/pdf/10.1002/cphc.201200021>.
- ⁴⁹ C. Katan, F. Terenziani, O. Mongin, M. H. V. Werts, L. Porrs, T. Pons, J. Mertz, S. Tretiak, and M. Blanchard-Desce, *The Journal of Physical Chemistry A* **109**, 3024 (2005), pMID: 16833626, <https://doi.org/10.1021/jp044193e>.
- ⁵⁰ C. Katan, F. Terenziani, C. L. Droumaguet, O. Mongin, M. H. V. Werts, S. Tretiak, and M. Blanchard-Desce, in *Linear and Nonlinear Optics of Organic Materials V*, Vol. 5935, edited by M. Eich, International Society for Optics and Photonics (SPIE, 2005) pp. 13 – 27.
- ⁵¹ L. G. Lukasiewicz, M. Rammo, C. Stark, M. Krzeszewski, D. Jacquemin, A. Rebane, and D. T. Gryko, *ChemPhotoChem* **4**, 508 (2020), <https://chemistry-europe.onlinelibrary.wiley.com/doi/pdf/10.1002/cptc.202000013>.
- ⁵² W. Kim, T. Kim, S. Kang, Y. Hong, F. Wrthner, and D. Kim, *Angewandte Chemie International Edition* **59**, 8306 (2020), <https://onlinelibrary.wiley.com/doi/pdf/10.1002/anie.202005696>.